Journal of Advanced Zoology

ISSN: 0253-7214

*Volume **44** Issue **S-6 Year 2023** Page **124:140***

Protective Role of Nanocurcumin in Cyclophosphamide-induced Cardiac Toxicity in Adult Male Albino Rat: A Histological, Immunohistochemical, Biochemical Study

Hafiz Waly Ahmed*, Hanan Nabih Gad-Allah, Sarah Mahmoud Kaooh, Hend Ahmed Mohamed Hussein, Tarek Ibrahim Abd El-Galil

Department of Anatomy and Embryology, Faculty of Medicine, Cairo University.

Corresponding Author: Hafiz Waly Ahmed

Article History

Received: 18 June 2023
Revised: 16 Sept 2023
Accepted: 22 Nov 2023

Abstract

Background: *Cyclophosphamide (CYP) is a cardiotoxic agent with antineoplastic and immunosuppressive properties. Objectives: To detect the histological, immunohistochemical, biochemical cardiac toxicity of CYP and determine the protective effectiveness of nanocurcumin on the cardiac muscle of albino rats.* ***Material and methods:*** *The current work used forty Wistar rats allocated into four groups; normal control (I), sham control (II), CYP-treated (III) and concomitant protective CYP + nanocurcumin (IV).* ***Results:*** *CYP-treated group (III) showed fragmented, disrupted cardiac myocytes with cellular infiltrates and interstitial edema. Blood vessels were dilated congested. Cardiac myocytes showed pyknosis, vacuolations and some showed karyolysis. Much improvement was observed in group IV. The area percentage of fibrous tissue, TNF-α and iNOS immunoreactivity in CYP-treated group III showed statistically significant increase in contrast to that of the control group. Use of nanocurcumin in groups IV ameliorate these changes. Biochemically, there were significant increase in means of CK-MB, cTn-1, MDA, levels and decrease of GPx activity in group III (CYP -treated group) compared to the control group. Uses of nanocurcumin has been observed to improve these changes .* ***Conclusion:*** *Cyclophosphamide (CYP) had deleterious effects on the histological structure of the heart, cardiac enzymes, collagen fibers deposition and myofibroblast proliferation in albino rats. Administration of nanocurcumin with CYP injection could largely ameliorate these changes .*

Keywords: *Cyclophosphamide, Nanocurcumin, Cardiac Toxicity, Albino Rat.*

1. Introduction

Cyclophosphamide (CYP) is a cytotoxic agent with strong antitumour properties. It is feasibly the most used anticancer drug. It is also used at a lower dose for treatment of non-neoplastic diseases such as rheumatoid arthritis 1. However, because CYP can harm normal tissues, leading to multiple organ toxicity mostly affecting the heart, testes, and bladder, its clinical application has been limited 2

The incidence of fatal cardiomyopathy with CYP ranges from 2.0% to 17.0%. CYP-induced cardiomyopathy happens in the first two or three weeks of treatment, as opposed to cardiomyopathy that develops months or years after high cumulative doses of anthracyclines 3.

The CYP pathogenesis involves direct endothelial damage causing increased permeability, microthrombosis and escaping of plasma proteins and erythrocytes into the myocardium 3.

Also, CYP causes rise in free oxygen radicals and impairs the heart's antioxidant defence system and heart lipoprotein lipase secretion. Furthermore, it has been documented that CYP caused its acute cardiotoxicity by uncoupling of mitochondrial-linked ATP synthesis 4.

Curcumin taken from Curcuma longa L. (Zengiberaceae family) roots, has been used for centuries in traditional medicine. It has demonstrated a variety of pharmacological and physiological and properties. It is commonly used in food coloring and as a spice and. It is thought to be safe and is recognised to have immunomodulatory, anti-inflammatory, and antioxidant properties 3.

Numerous research has been suggested the protecting role of curcumin in contradiction of oxidative stress-mediated nephropathy, cardiomyopathy, neuropathy, and hepatic injury. However, numerous obstacles restrict the clinical application of curcumin as its chemical instability, poor aqueous solubility, photodegradability, fast metabolism, and short half-life reducing its bioavailability when it is taken 5.

Curcumin delivery systems that include oil, surfactant/co-surfactant, and an aqueous phase are known as nano-emulsions, and they are highly promising. It increases its bioavailability up to 9 folds leading to better pharmacokinetic profile maximizing its protective & therapeutic potentials 6.

The protecting effect of such nanocurcumin in cardiotoxicity caused by CYP has not been investigated before thus the present study is aiming to assess this effectiveness on adult male rats.

2. Material and Methods

Animals

In the current investigation, fifty mature male Wistar strain albino rats weighing 200–250g were utilised. After receiving approval from the Institutional Animal Care and Use Committee (CU-III-F-8-21), rats were acquired from the Animal House, Faculty of Medicine, Cairo University. Before beginning the experiment, they spent two weeks getting used to the lab environment. They were fed regular rat chow, bred in wire mesh cages with five rats per cage, kept at a constant temperature of 24 ± 1°C, and had a regular cycle of light and dark. Food and water were always available to the animals.

Chemicals

- Cyclophosphamide: It was achieved from Baxter Oncology (Düsseldorf, Germany) as powder in the form of 1gm vials diluted in 10 cm saline.
- Nano Curcumin: It was bought from Nanotech Egypt for photo-Electronics as powder of brown-yellow color.

Preparation of curcumin Nano emulsion:

Curcumin Nano-emulsion was prepared from ethanol extract, acquired from local market, of common powder of curcumin longa root. The later was prepared by mixing 200g simple powder of rhizome in 800 ml of 98% ethanol mixing them on a high speed. At room temperature, the liquid phase evaporated in the petri dishes. The resulting powder was stored at room temperature in a sterile bottle glass until it was used to prepare the Nano emulsion. The oil phase of the ethanol extract was mixed with an aqueous phase that contained phosphate buffer solution at PH 7, 10% (v/v) Tween 80 (based on the oil phase), and 4% and 10% dissolved maltodextrin to create an oil water curcumin nano-emulsion, Afterward, to ensure thorough hydration, the mixture was stirred for at least 15 minutes using a fast speed (20000 rpm) magnetic stirrer. An emulsion that is stable having a 20% ethanol extract of curcumin was the result.

Nano-emulsion specifications

The previously mentioned procedure was used to create the curcumin nano-emulsion. The prepared nano-emulsion's particle size was 14.3-25.5 nm. Measurement of the particle size was established using Transmission Electron Microscope (TEM) (Fig.1).

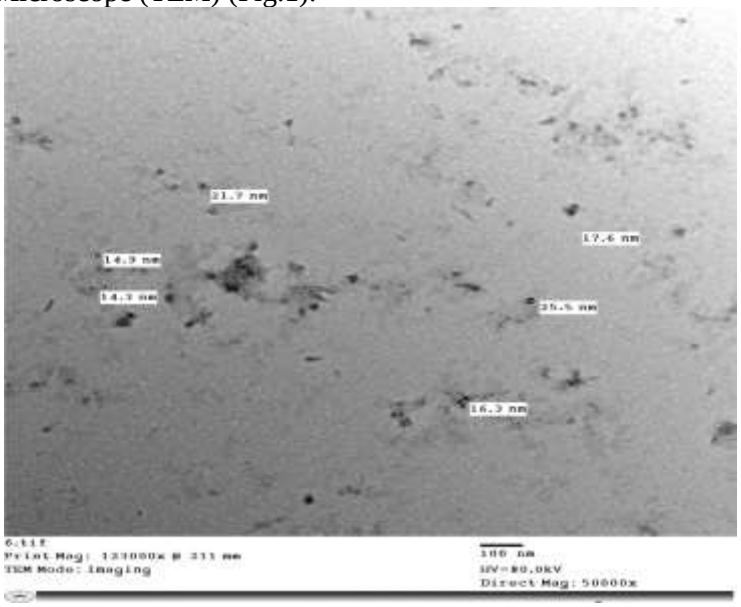

Fig. (1): Size characterization of curcumin nanoparticles by TEM

Methods

The rats were divided randomly into four groups, ten rats each: Group I (normal control): rats did not obtain any medication. Group II (sham control): the rats administrated a single dosage of physiological saline (solvent of CYP) 2 ml/kg injected intraperitoneally (i.p). Group III (CYP-treated group): the rats were given a single dose of CYP 200 mg/kg, i.p. **.**Group IV (concomitant protective CYP + nanocurcumin): rats got a single dose of CYP 200 mg/kg, i.p and concomitantly receive nanocurcumin 5 mg/kg, i.p daily for 2 weeks.

As the conclusion of the testing period approaches, rats were sacrificed after 2 weeks and hearts were extracted, plotted dry on filter paper. Two specimens were taken from the left ventricle, one of them fixed in Ten percent formalin solution for light microscopy and immunohistochemical studies. The other specimen was prepared for biochemical (Creatine phosphokinase-MB (CK-MB), cardiac troponin-1(cTn-1), Glutathione peroxidase (GPx) and Malondialdehyde (MDA)

Light Microscopic Examination

After routine paraffin processing, the light microscopic study was carried out using Hematoxylin and Eosin (Hx &E), Masson's trichrome stain and immunohistochemical staining using the mouse anti-rat monoclonal antibody for Tumor necrosis factor- alpha (TNF-α) for detection of inflammation and Inducible nitric oxide synthase (iNOS) antibody for detection of oxidative stress. Detection System for antibodies by immunostaining was carried out using the Histostain SP kit (LAB-SA system, Zymed Laboratories Inc, San Francisco, USA, 95-9643). It is a broad-spectrum detection device that reacts with primary antibodies from mice, rabbits, guinea pigs, and rats. A horseradish peroxidase streptavidin, a biotinylated secondary antibody, serum blocking solution, and a substrate chromogen combination are all included in this Histostain SP kit to show antigen in cells and tissues.

Histomorphometric Studies

Histomorphometric estimation of the area percentage of TNF- α and iNOS immunoreactivity as well as the are percentage of collagen in masson's trichrome-stained sections was performed using the "Leica Qwin 500 C" image analyzer computer system Ltd., quantitative data were gathered (Cambridge, England). The image analyzer was made up of a coloured video camera, a coloured monitor, an IBM personal computer's connected to the microscope is a hard drive, and "Leica Qwin 500 C" software to control it.

Biochemical study

Each animal's heart was divided into smaller pieces, which were then prepared in 0.1M phosphate buffer saline solution and spinning at 1200 rpm for 10 minutes. The following conclusions were drawn from the supernatant:

Creatine kinase isoenzyme-MB (CK-MB) activities

For detection of myocardial injury, a diagnostic marker enzyme, creatin kinase isoenzyme-MB (CK-MB) was used 7. Tissue analysis was performed using ELISA using the Roche/Hitachi Cobas c 701 system to measure the CK-MB. According to the produce, readily accessible test reagents were used for each step of the immunological UV test. The two subunits, CK-M and CK-B,make up the CK-MB isoenzyme. The CK-M subunit's catalytic activities were 99.6% inhibited in the sample with the aid of CK-M-specific antibodies, while the CK-B subunit remained unaffected. The total CK method was used to measure the CK-B activity, which is equal to half of the CK-MB activity.

Cardiac troponin-1 (cTn-1)

Using the VIDAS Troponin I Ultra kit, the enzyme-linked fluorescence assay was used to quantify the levels of troponin I. The kit's readily available test reagents were used to run the test in the VIDAS apparatus entirely autonomously. The material was added to the well containing anti-cardiac troponin I antibodies labelled with alkaline phosphatase (conjugate). To assure the uniting of the antigen to the conjugate and troponin I, the sample-conjugate mixture was added to the container. The unrestrained content was removed by flooding. The substrate, 4-methyl umbelliferyl phosphate, is hydrolyzed by the attached enzyme to 4-methylumbelliferone. The antigen concentration in the sample directly correlates with the fluorescence intensity.

Glutathione peroxidase (GPx) activity

Examination of tissue antioxidant enzyme activities 8. The techniques in accordance with the instructions provided by the manufacturer (LAB-SA system, Zymed Laboratories Inc, San Francisco, USA, 95-9643). The xanthine/xanthine oxidase system's suppression of nitrobluetetrazolium breakdown by O2 is utilized as a stand-in for evaluating the enzyme activity in tissue homogenate. The amount of enzyme causing 50% inhibition in 1 mL of reaction solution per gramme of tissue protein was defined as the GPx activity unit, and the result was stated in nmol/mg of tissue.

Malondialdehyde (MDA) level

For examination of tissue antioxidant enzyme, Malondialdehyde (MDA), a byproduct of lipid peroxidation, is used to assess how much oxidative stress is present in a tissue. Biodiagnostics provided the test supplies for this procedure in the form of kits. The most crucial component of this procedure was the addition of thiobarbituric acid (TBA) to sodium sulphate, trichloroacetic acid, and TBA to the tissue homogenate. The mixture was then treated for 30 minutes in a bain-marie of boiling water. After extracting the chromogen, the organic phase's sensitivity was estimated at 530 nm. MDA (mmol/mg tissue), used as the reference standard, was used to measure the results 8.

Statistical analysis

Statistical Package for Social Science (SPSS) version 21 was employed to statistically examine the numerical data of the biochemical levels and histomorphometric measurements. The information was displayed as mean standard deviation (SD). Two-tailed one-way analysis of variance was applied. For each experimental group, the standard deviation and the P value were computed and then compared between the various groups. The Kolmogorov-Smirnov test was used to check the quantitative data for normalcy. P-values of 0.05 or less were regarded as significant.

3. Results and Discussion

Histological observation

The cardiac myocytes of the control groups stained with H&E showed well organized, anastomosing, and branching cardiac muscle fibers, running almost longitudinally with minimal spacing (Fig.2). Sections of group III (CYP-treated rats) showed extensive loss of normal architecture of the myocardium in the form of fragmented, disrupted and widely separated cardiac muscle fibers with irregular wavy cardiac muscle fibers were seen in some areas. Some fibers have deeply stained sarcoplasm (Fig. 3).

In addition, thick-walled blood vessel was observed (fig.4). Extravasation of blood was detected (figs. 3 & 5). Moreover, dilated congested blood vessels and inflammatory cellular infiltrates were also noticed perivascular and in between the cardiac muscle fibers. Some cardiac myocytes showed pyknosis others with vacuolations (Fig.5).

Furthermore, some cardiac myocytes showed karyolysis, in addition to interstitial edema (Fig.6).

The cardiac muscle fibers in group IV showed apparently normal architecture of myocardium with regular branching and anastomosing cardiac muscle fibers. Narrow interstitial spaces with minimal cellular infiltrates (CL) are also seen.

(Fig. 7). The collagen fibers were few in the control group (Fig.8). Marked collagen deposition between irregularly degenerated cardiac muscle fibers and around the blood vessels was seen in group III (Fig. 9). There was a moderate amount of interstitial collagen deposition in group IV (Fig. 10).

The immunoreactivity of TNF-α was minimal positive in group I in the form of brown discoloration in the myocardium (Fig.11), while there was marked positive immunoreactivity in group III (Fig.12). In group IV there was moderate positive immunoreactivity (Fig.13).

The immunoreactivity of iNOS-stained sections of control groups showed almost negative immunoreactivity in the myocardium in the form of absent brown discoloration (Fig.14), while in group III it showed marked positive immunoreactivity in the myocardium as brown discoloration in the myocardium (Fig.15). In group IV there was moderate positive immunoreactivity (Fig. 16).

Biochemical study

Mean CK-MB Level & Mean Cardiac troponin-1 (cTn-1) (Table 1& 2)

The mean values of CK-MB activities & (cTn-1) levels were significantly increased in group III relative to control groups. On the other hand, there was significant reduction of CK-MB activities & (cTn-1) levels in group IV relative to group III. However, there was a significant rise in CK-MB activities and non-significant increase in (cTn-1) levels groups IV in contrast with the control groups.

Mean Glutathione peroxidase (GPx) activity (Table 3)

The mean values of GPx activity were significantly decreased in group III in contrast with control groups. However, there was significant increase of GPx activities in groups IV as compared to that of group III. However, there was a significant reduction in groups IV in contrast with the control groups.

Mean Malonaldehyde (MDA) (Table 4)

The mean values of MDA were significantly increased in group III in comparison with control groups. Significant reduction of MDA was observed in groups IV relative to group III. On other hand, there was a significant increase in groups IV in comparison with the control groups.

Histomorphometric study

The mean area percentage of collagen fibers in group III was significantly higher than the control groups. However, groups IV displayed a significant decrease in the mean area percentage of collagen fibers when compared to that of group III. Additionally, there was a non-significant rise in groups IV compared to the control groups (Table 5).

The mean area percentage of TNF-α (Table 6) and iNOS (Table 7) in group III displayed statistically significantly increase relative to the control groups. On the other hand, the area percentage of TNF-α and iNOS in groups IV showed significant reduction in comparison with similar values of group III. The mean value in groups IV showed statistically non-significant increase as compared to control groups.

Table (1): Mean ± SD of the creatinine kinase isoenzyme-MB (CK-MB) activities in cardiac tissue among different experimental groups:

Group	CK-MB activities in cardiac tissue (U/l) Mean ± SD
I	130.58±4.51#$
II	132.60±5.02#$
III	290.26±10.12+*$
IV	165.98±8.64+*#

Table (2): Mean ± SD of the cardiac troponin-1 (cTn-1) in cardiac tissue among different experimental groups:

Group	cardiac troponin-1 (ng/ml) in cardiac tissue Mean ± SD
I	0.138±.01#
II	0.150±.02#
III	0.632±0.05+*$
IV	0.274±0.03#

Table (3): Mean ± SD of glutathione peroxidase (GPx) activity in cardiac tissue among various experimental groups:

Group	Glutathione peroxidase (GPx) activity in cardiac tissue (nmol/mg ptn) Mean ± SD
I	117.26±6.35#$
II	115.08±7.59#$
III	42.60±2.77+*$
IV	98.44±5.98+*#

Table (4): Mean ± SD of MDA level in cardiac tissue among different experimental groups:

Group	MDA level in cardiac tissue Mean ± SD (mmol/mg ptn)
I	44.66±1.13#$

II	46.28±1.59#$
III	165±1.71+*$
IV	64.46±4.45+*#

Table (5): Mean± SD area percent of collagen fibers in cardiac tissue among various experimental groups:

Group	Area percent of collagen fibers in cardiac tissue Mean ± SD
I	2.830±0.488#
II	3.298±0.823#
III	20.634±1.413+*$
IV	4.306±0.888#

Table (6): Mean± SD area percent of TNF-α immunoreactivity in cardiac tissue among different experimental groups:

Group	Area percent of TNF-α immunoreactivity in cardiac tissue Mean ± SD
I	0.872±0.062#
II	1.174±0.085#
III	6.680±.925+*$
IV	2.380±0.149#

Table (7): Mean± SD area percent of iNOS immunoreactivity in cardiac tissue among different experimental groups:

Group	Area percent of iNOS immunoreactivity Mean ± SD
I	1.916±0.437#
II	2.376±0.889#
III	20.696±1.206+*$
IV	4.474±0.858#

SD= standard deviation
, + : significant versus group I, *: significant versus group II, #: significant versus group III, **$**: significant versus group IV.

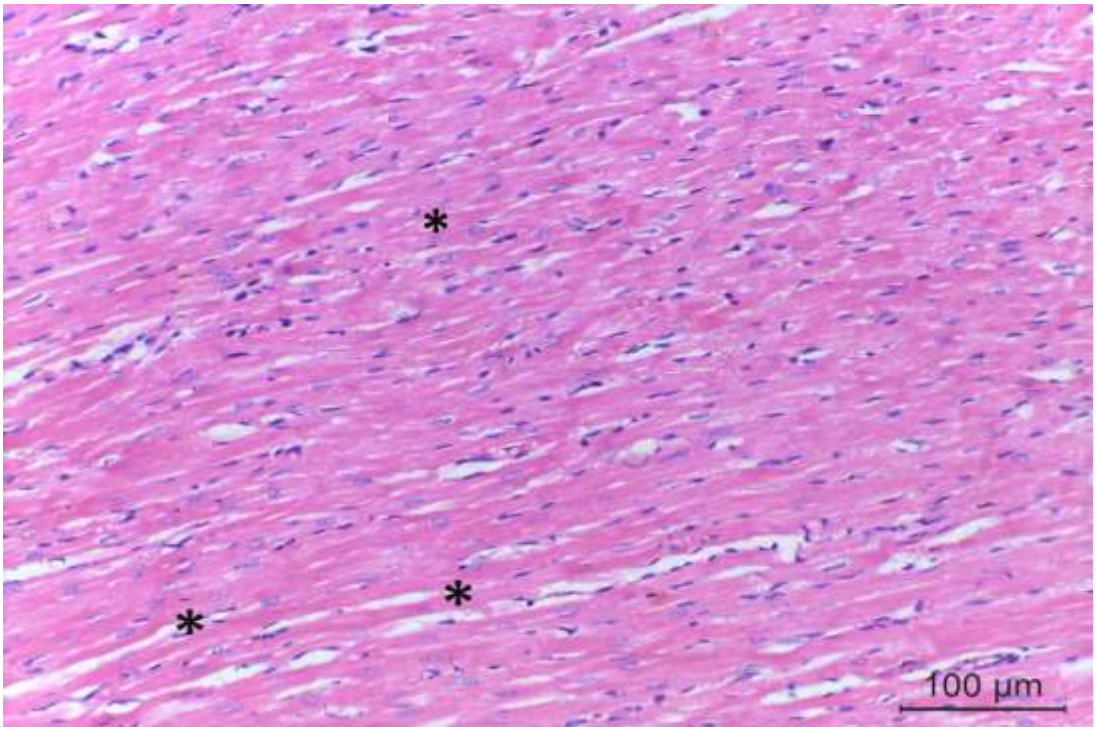

Fig. (2): Photomicrograph of a section in the left ventricle of a rat of control group (group I) showing, well organized, branching and anastomosing cardiac muscle fibers (asterisks), running almost longitudinally with minimal spacing.

(Hx&E X 400)

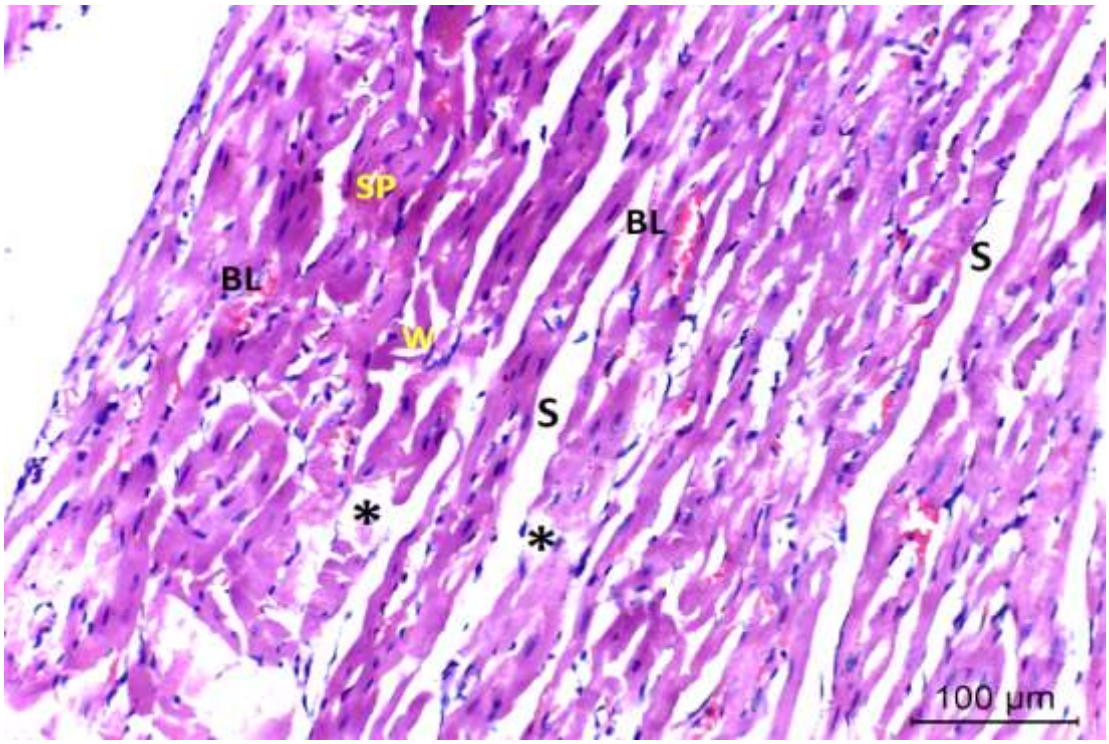

Fig. (3): Photomicrograph of a section in the left ventricle of a rat of CYP-treated group (group III) showing, extensive loss of normal architecture of myocardium. Fragmented, disrupted (asterisks) and widely separated cardiac muscle fibers (S). Irregular wavy cardiac muscle fibers were seen in some areas (W). Some fibers have deeply stained sarcoplasm (SP). Extravasation of blood can be detected (BL).

(Hx&E X 400)

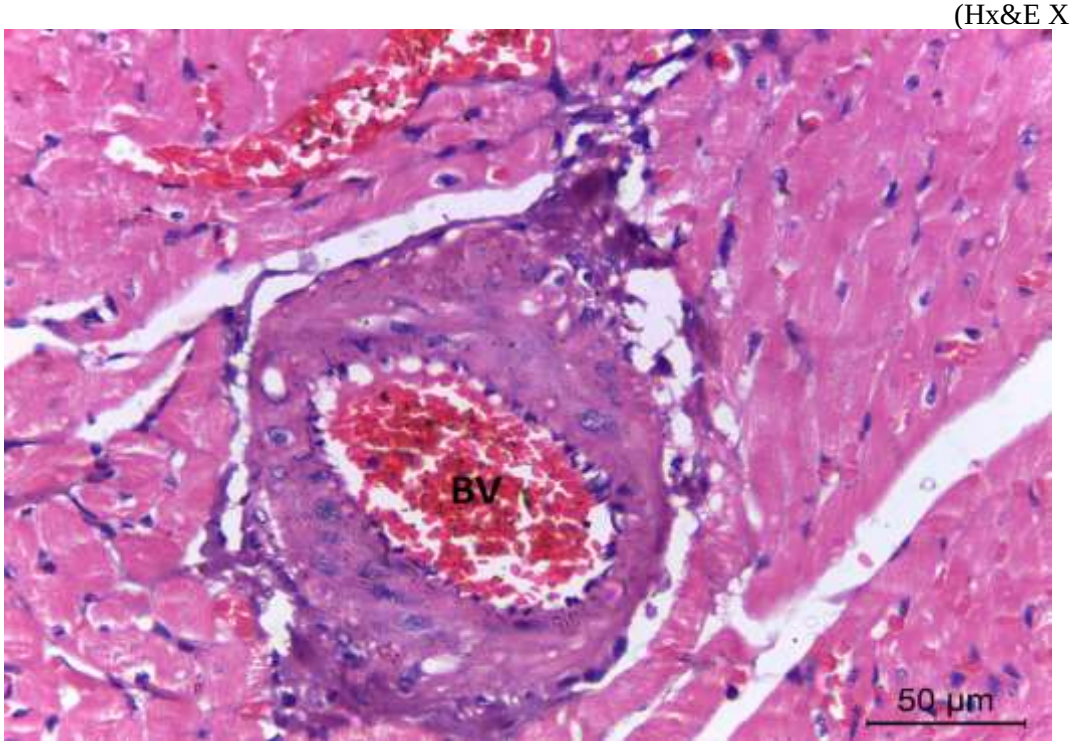

Fig. (4): Photomicrograph of a section in the left ventricle of a rat of CYP-treated group (group III) showing, thick-walled blood vessel (BV).

(Hx&E X 400)

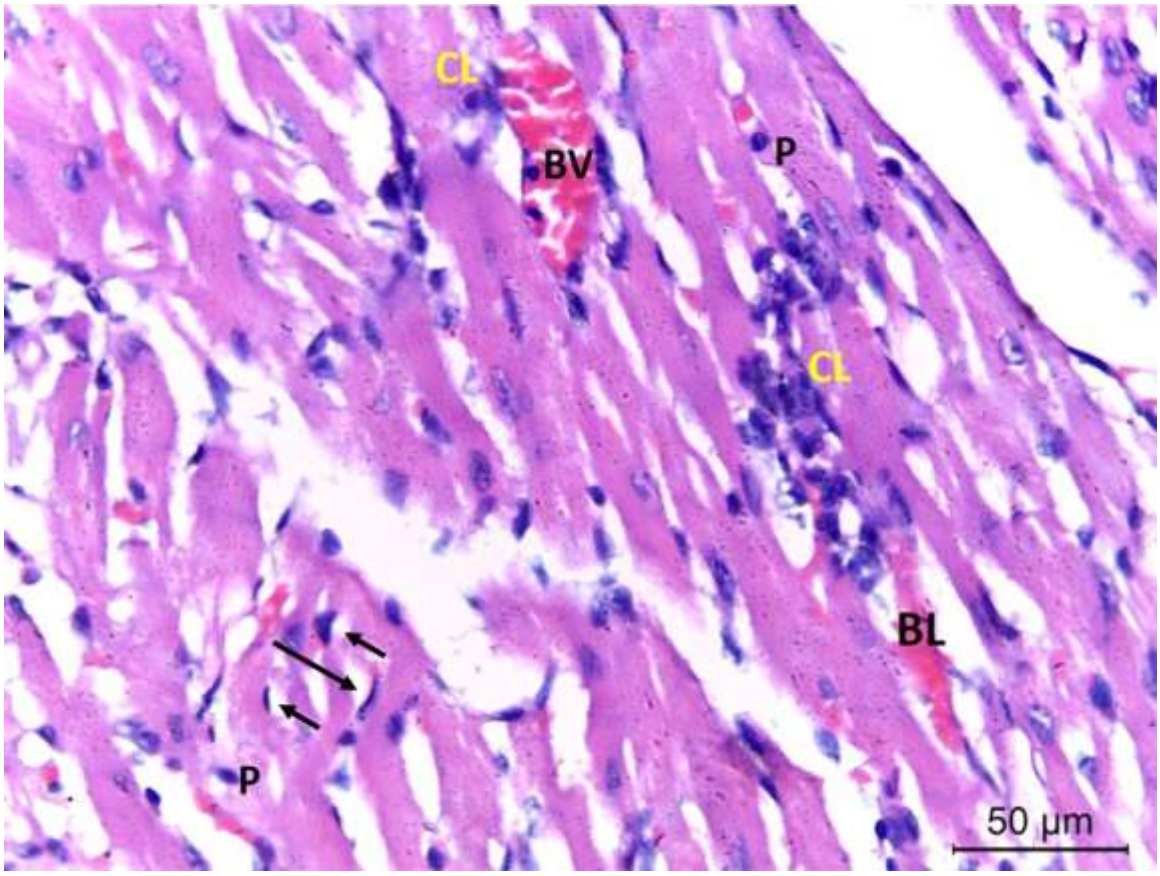

Fig. (5): Photomicrograph of a section in the left ventricle of a rat of CYP-treated group (group III) showing, congested blood vessel (BV) with extravasation of blood (BL). Inflammatory cellular infiltrates (CL) have been seen in between the cardiac muscle fibers and perivascular. Some cardiac myocytes with pyknosis (P), others with vacuolation (arrows).

(Hx&E X 400)

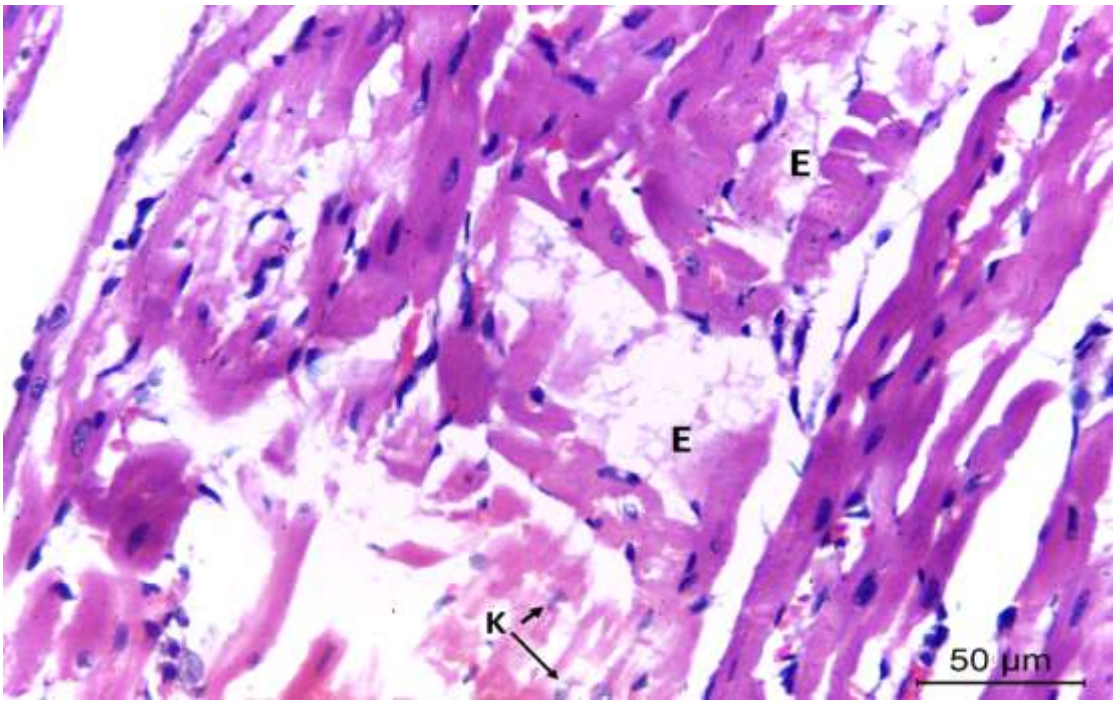

Fig. (6): Photomicrograph of a section in the left ventricle of a rat of CYP-treated group (group III) showing some cardiac myocytes with karyolysis (K). Interstitial edema (E) can also be detected.

(Hx&E X 400)

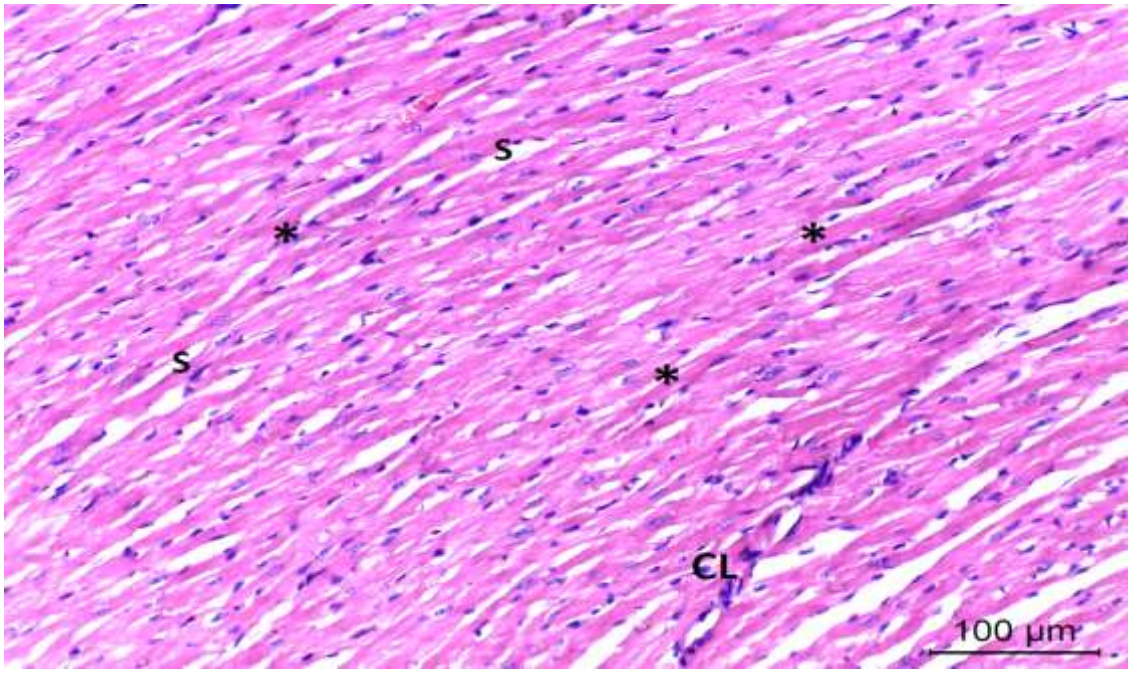

Fig. (7): Photomicrograph of a section in the left ventricle of rat of prophylactic protective nanocurcumin group (group IV) showing apparently normal architecture of myocardium with regular branching and anastomosing cardiac muscle fibers (asterisks). Narrow interstitial spaces (S) with minimal cellular infiltrates (CL) are also seen.

(Hx&E X 400)

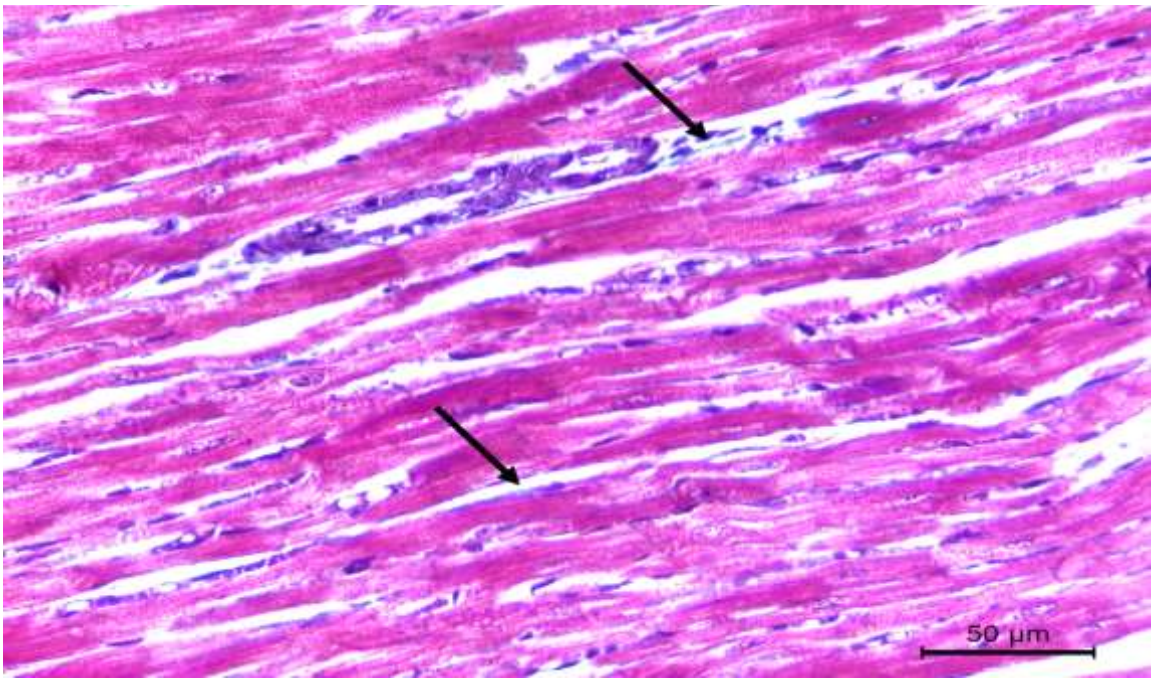

Fig. (8): Photomicrograph of a section in the left ventricle of a rat of control group (group I) showing, few amount of collagen fibers deposition.

(Masson's trichrome X 400)

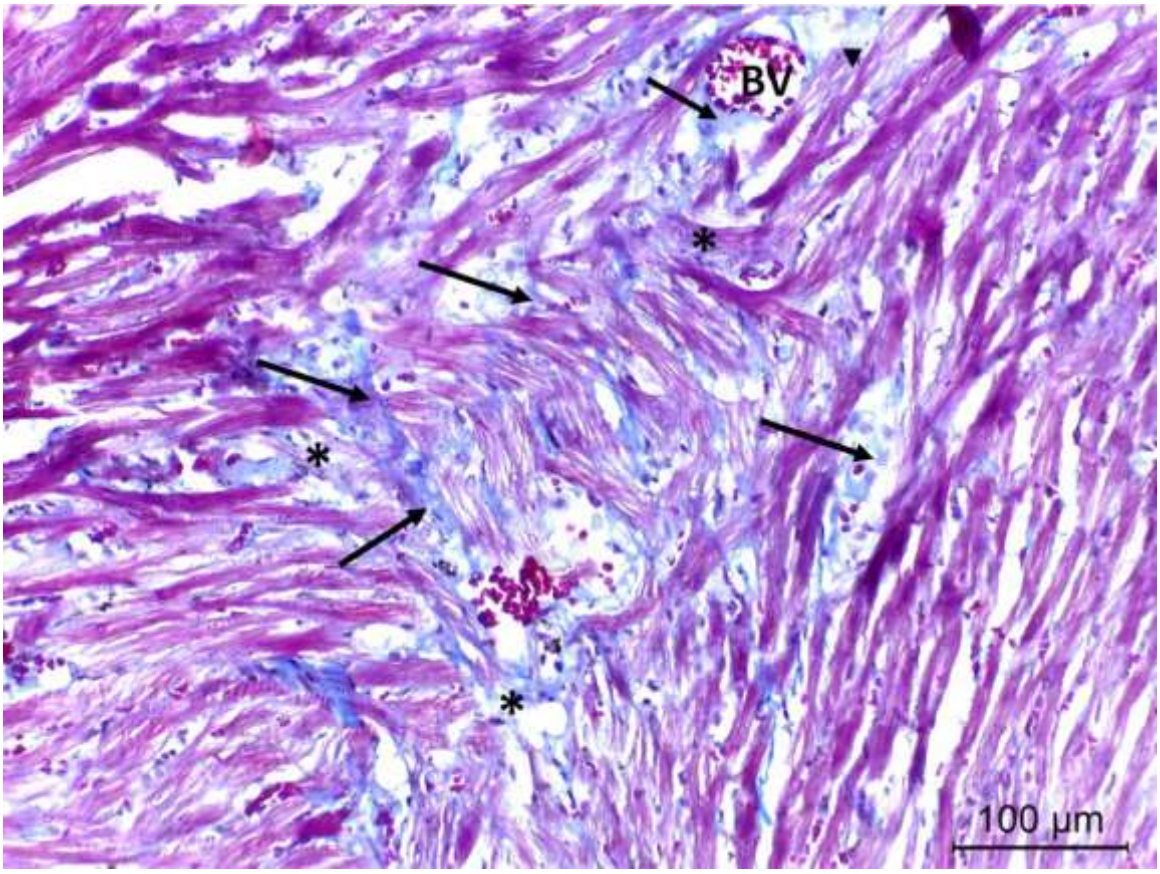

Fig. (9): Photomicrograph of a section in the left ventricle of a rat of CYP-treated group (group III) showing, marked collagen deposition (arrows) between irregularly degenerated cardiac muscle fibers (asterisks) and around the blood vessels (BV).

(Masson's trichrome X 200)

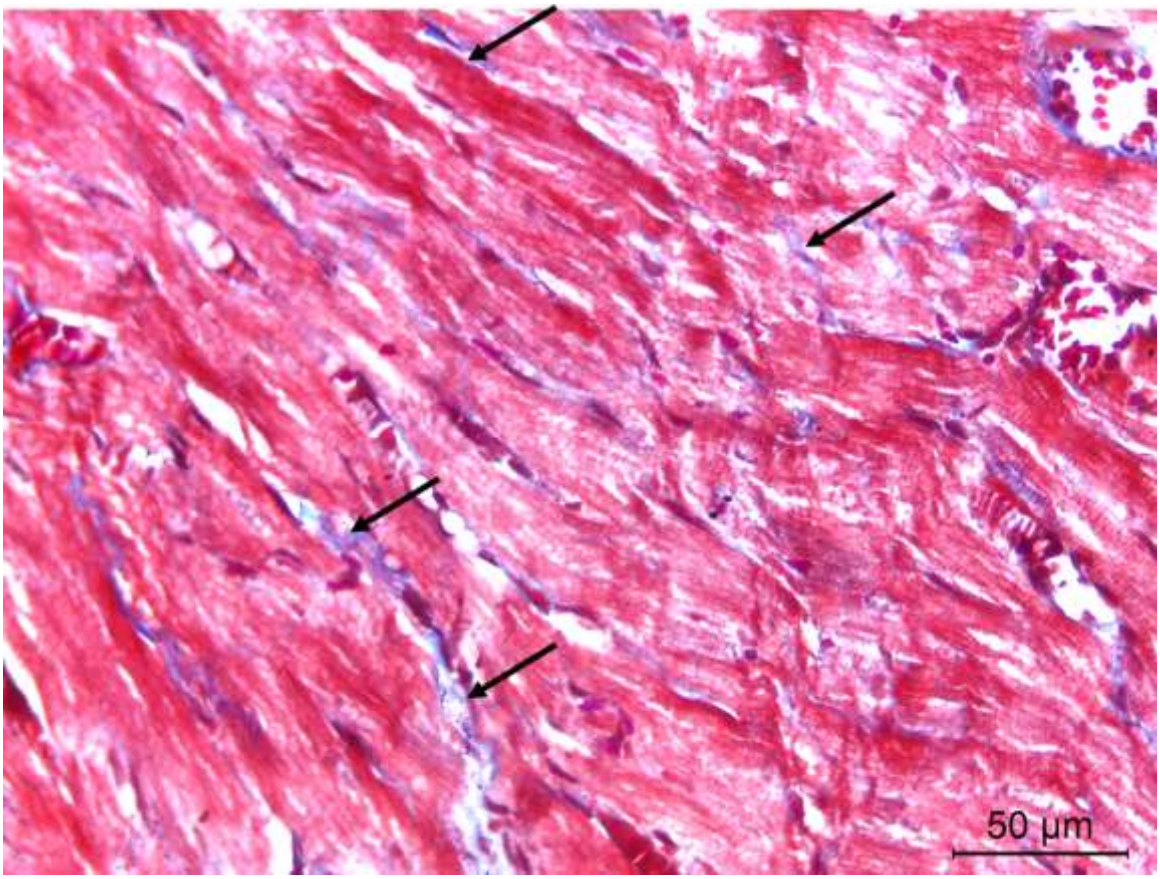

Fig. (10): Photomicrograph of a section in the left ventricle of a rat of concomitant protective nanocurcumin group (group IV) rat showing, moderate amount of interstitial collagen fibers deposition between cardiac muscle fibers.

(Masson's trichrome X400)

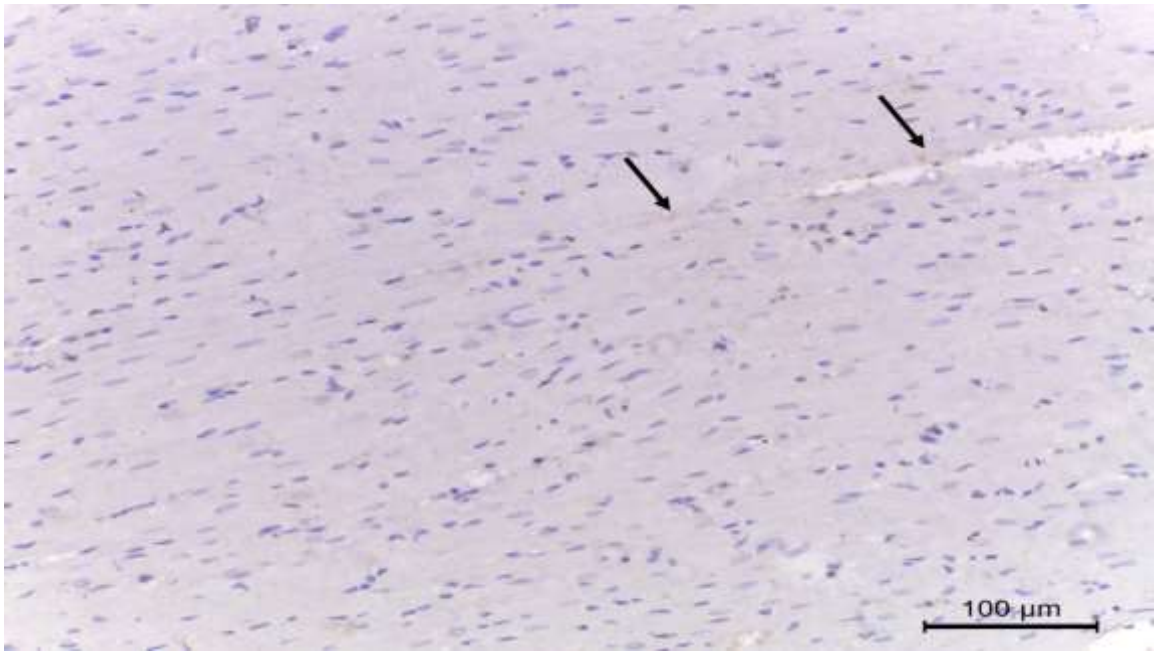

Fig. (11): Photomicrograph of a section in the left ventricle of a rat of control group (I) showing, minimal positive immunoreactivity as brown discoloration in the myocardium (arrows).

(TNF-α X 200)

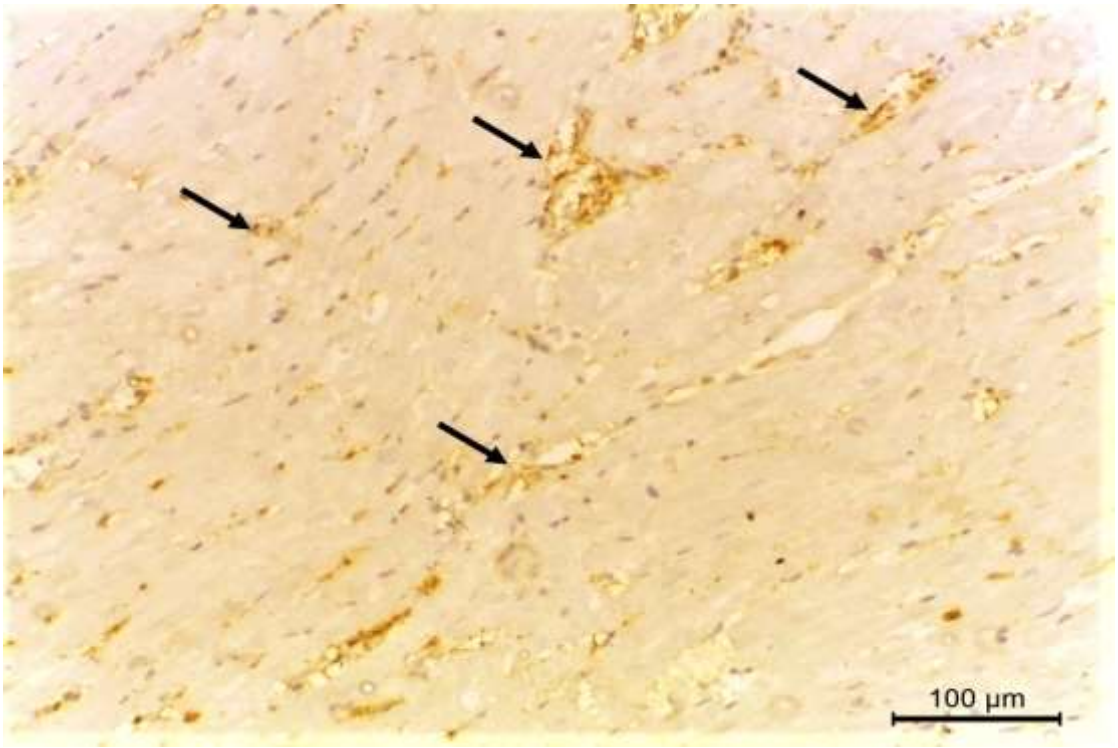

Fig. (12): Photomicrograph of a section in the left ventricle of a rat of CYP-treated group (group III) showing, marked positive immunoreactivity as brown discoloration in the myocardium (arrows).

(TNF-α X 200)

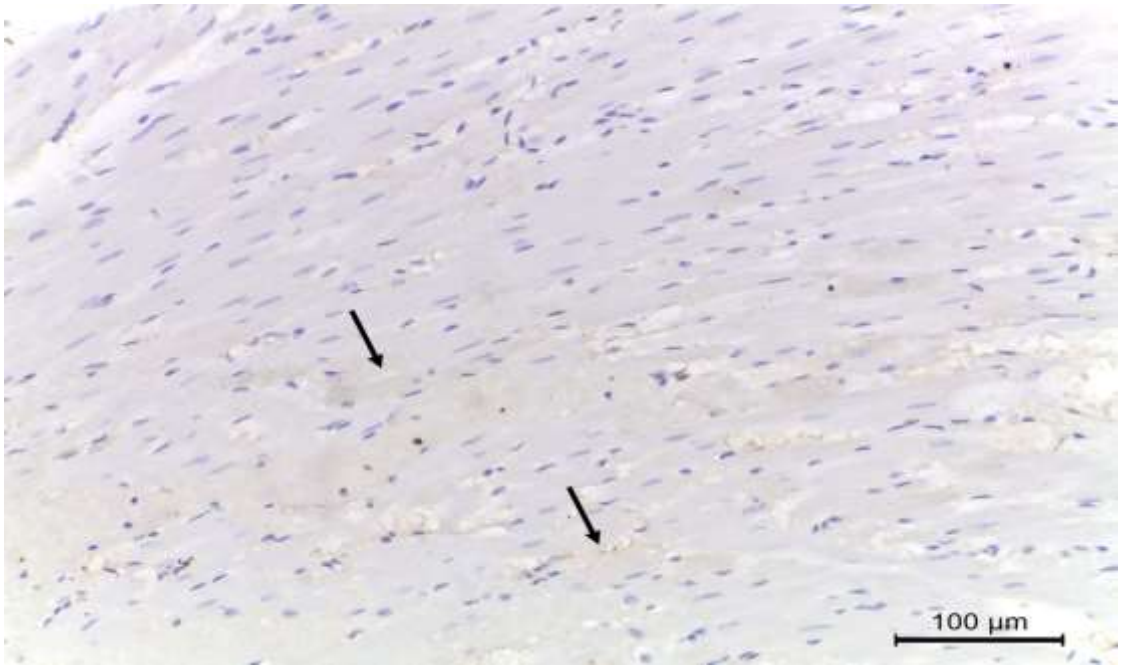

Fig. (13): Photomicrograph of a section in the left ventricle of rat of prophylactic protective nanocurcumin group (group IV) showing, minimal positive immunoreactivity as brown discoloration in the myocardium (arrows).

(TNF-α X 200)

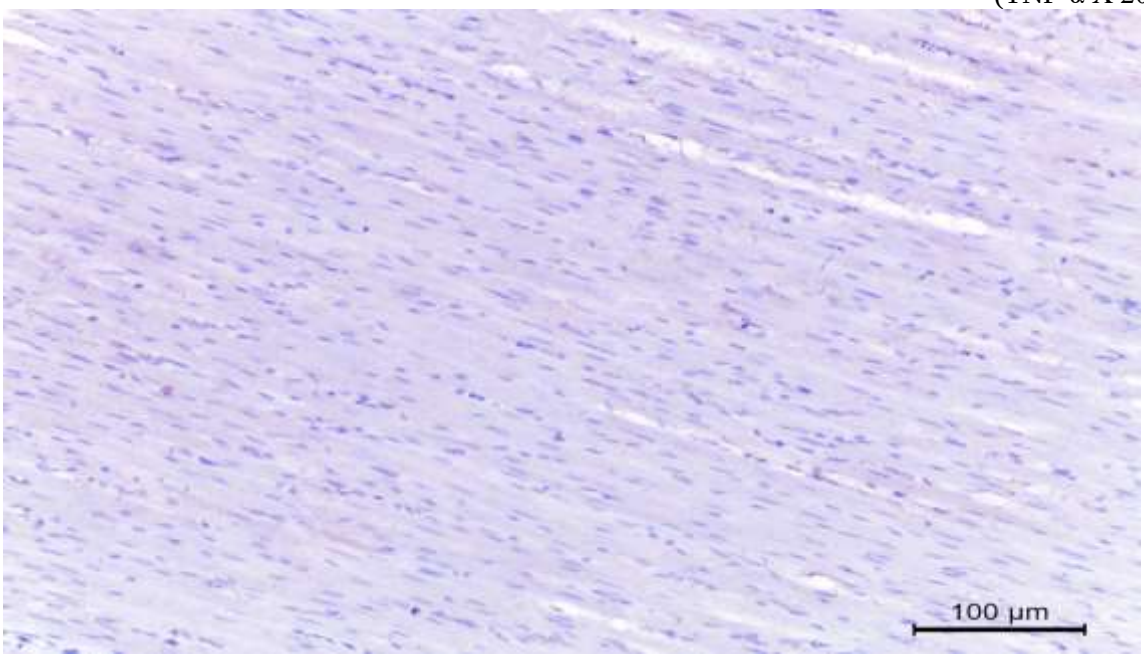

Fig. (14): Photomicrograph of a section in the left ventricle of a rat of control group (I) showing, almost negative immunoreactivity in the myocardium in the form of absent brown discoloration.

(iNOS X 200)

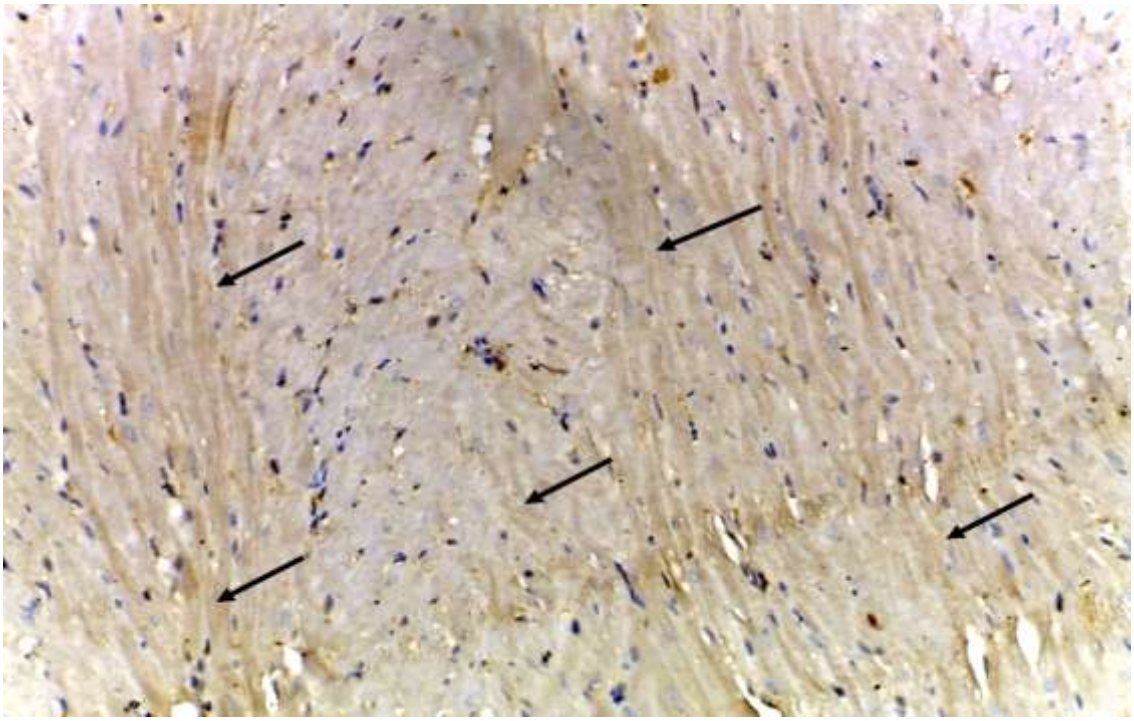

Fig. (15): Photomicrograph of a section in the left ventricle of a rat of CYP-treated group (group III) showing, marked positive immunoreactivity as brown discoloration in the myocardium (arrows).

(iNOS X 200)

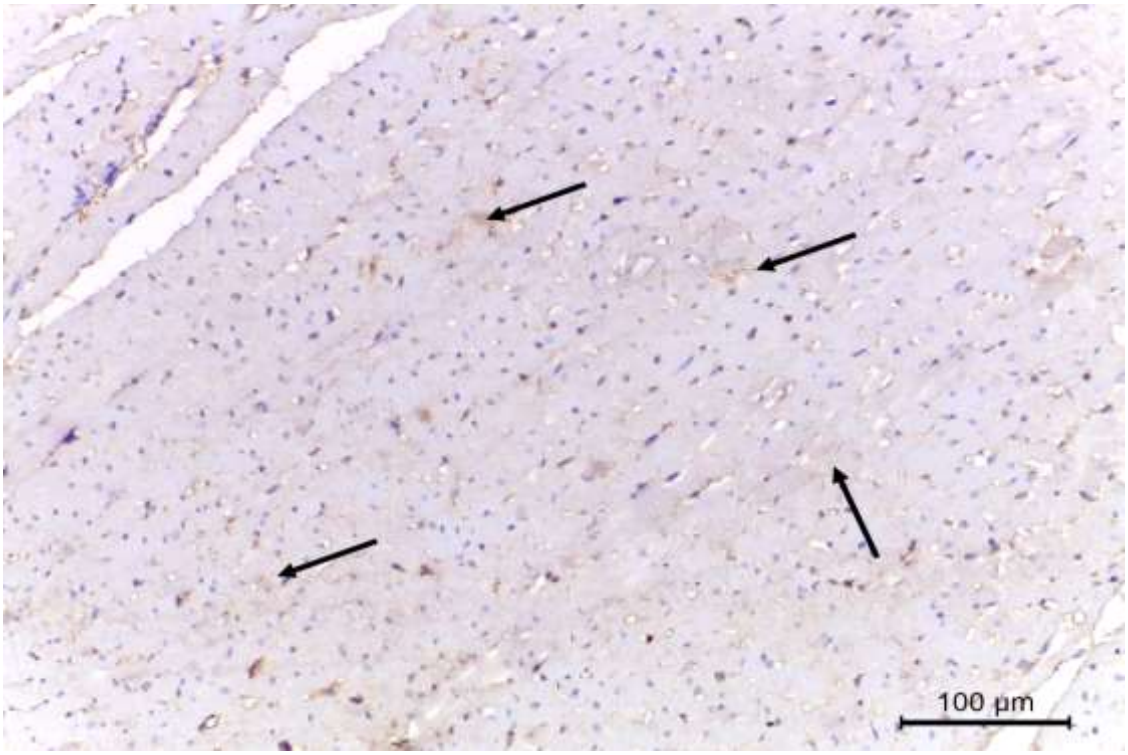

Fig. (16): Photomicrograph of a section in the left ventricle of a rat of concomitant protective nanocurcumin group (group IV) showing, moderate positive immunoreactivity in the myocardium as brown discoloration in the myocardium (arrows).

(iNOS X 200)

In cancer patients, CYP dramatically worsens cardiac outcomes. Thus, there is an urgent need to create strategies that can both effectively prevent CYP-induced cardiotoxicity and continue to have anticancer effects. The current study showed that nanocurcumin protects the heart from CYP-induced cardiotoxicity. This is probably due to its antioxidation, anti-inflammation and anti-apoptotic activities3.

In the current work, Hematoxylin and Eosin-stained sections of CYP-treated rats (group III) exhibited extensive histological changes as an example of loss of normal architecture of myocardium with fragmented, disrupted and widely separated cardiac muscle fibers. Also, fibers of extremely stained sarcoplasm can be detected. These previous results agree with) 3, 9 &10 who attributed that CYP induces toxicity through its toxic metabolite, acrolein, that causes oxidative injury and discharge of some inflammatory mediators as nitric oxide (NO) and cytokines.

Another finding was areas of irregular waviness of cardiac muscle fibers, this finding agrees with 9 &10. The wavy myofibers was account for spasm or contraction of the broken fibers 10.

Additionally, the myocardium of CYP-treated rats (group III) showed excess cellular inflammatory infiltration among the cardiac muscle fibers and perivascular. Similar outcomes were reported by 3 &11. The cellular infiltration is due to excess production of reactive oxygen species 3. Additionally,11 correlated the inflammation activity with the expression of TNF-α and IL-1.

Also, there was vacuolation in some cardiac myocytes. This finding is in alignment with, 12, 9 & 10. This could be due to direct damage of CYP to the myocardial endothelium causing death of myocardial cells 12. CYP increases the oxidative stress resulting in mitochondrial injury and dysfunction with depletion of ATP leading to swelling of mitochondrial organelles 9.

Another finding in CYP-treated rats (group III), was cardiac myocyte degenerative changes in the form of pyknosis and karyolysis. These findings agree with 13&9. The authors 13 attributed that to the decreased level of GSH, that protects the cardiac cells from reactive oxygen species, resulting in increased oxidative stress with subsequent cell damage as well as cytoskeletal proteins damage as mentioned 9.

Furthermore, dilated congested blood vessels with subsequent blood extravasation and edema were observed in CYP-treated rats (group III). These findings may be due to the injury of vascular endothelial caused by CYP which resulting in leakage of blood and fluid into the myocardium 3. El-Agamy and his colleagues 14 also attributed that to the increasing level of inflammatory mediators and oxidative stress that rises heme-oxygenase formation leading to oxidative vascular endothelial cell injury.

Moreover,blood vessels with thickened wall were detected in the myocardium of CYP- treated rats (group III). This is in accordant with 15 who attributed the thickening of blood vessel wall to the tunica media cellular proliferation.

Another finding in the CYP-treated rats (group III), was the highly significant rise in the mean area percent of collagen fibers deposition in the myocardium and around the blood vessels as related to the control groups. This finding agrees with 16 & 10. This change could be attributed to the production of fibrotic and inflammatory mediators affecting the integrity and function of myocardial cell membranes and increasing the turnover leading to pathological remodeling of the extracellular matrix protein increasing its deposition and fibrosis 10.

the mean area percent of TNF-α stained sections of CYP-treated rats (group III) revealed significantly high positive immunoreactivity in the myocardium compared to the control groups. CYP activates the proinflammatory cytokines and results in the stimulation of NF-κB which results in expression of NO, TNF-α and other proinflammatory mediators that have a crucial role in heart inflammation 4.

Furthermore, it was found that the mean area percent of iNOS stained sections of CYP-treated rats (group III) showed significantly high positive immunoreactivity in the myocardium compared to the control groups. This outcome agrees with the work carried out by 4 & 17. According to the authors, hypoxia resulting from CYP-induced cardiac dysfunction led to an increase in iNOS production. This production may have been facilitated by the transcriptional factor for iNOS called hypoxia inducible factor-1α gene expression (HIF-1α).

Biochemically, the current investigation founded a significant rise in mean CK-MB & cTn-1 in CYP-treated rats (group III) compared to control groups. This finding is like those detected by 12 & 1. These finding could be explained by the direct injury to myocardial endothelium, thus causing death of myocardial cells and leakage of cardiac enzymes into the interstitium 12. In addition,10 attributed that to the increase in cell membrane permeability or myocytes necrosis due to the oxidative damage effect of CYP with subsequent cardiac enzymes leakage.

Also, the investigations founded that there was a statistically significantly decrease of the mean GPx level in hearts of CYP-treated rats (group III). This result was agreed with those found by 18. The

authors reported that free radicals generated during uding CYP resulting in consumption of GPx with subsequent increase in oxygen free radicals leading to oxidative stress and cell membrane injury,

The mean values of MDA were significantly raised in CYP-treated rats in contrast to control groups. This might be because the generation of free radicals and lipid peroxidation 3.

The current research detected that the use of nanocurcumin ameliorated the deleterious effect of CYP.

Hematoxylin and Eosin-stained sections of group IV showed apparently normal construction of myocardium with regular anastomosing and branching cardiac muscle fibers and narrow interstitial spaces.

The protective effect of nanocurcumin may be counted for its antioxidant properties as reported by 19 who assumed that nanocurcumin increases the levels of superoxide dismutase, antioxidants, and glutathione thus cleaning the reactive oxygen and nitrogen species and protecting the endothelial cells from oxidative damage. Also, nanocurcumin reduces lipid peroxidase levels in the myocardium 20.

The protective influence of nanocurcumin may be also because of its antiapoptotic activates as mentioned by 21 who reported that nanocurcumin acts as TNF-α antagonist stopping its role in apoptosis.

Moutabian and his colleagues 22 added that nanocurcumin reverses the necrosis and apoptosis by decreasing the NF-κB which stimulate the production of pro-apoptotic genes.

Furthermore, In the current work, nanocurcumin improved the cardiac edema and blood extravasation in group IV compared to group III. This improvement could be attributed to the anti-inflammatory effects of nanocurcumin as mentioned by 23 who clarified that nanocurcumin enhances nitric oxide formation by reducing oxidative stress thus improving endothelium-dependent vasodilation.

In the current research, there was decrease in the level of cellular inflammatory infiltrate in group IV compared to CYP group III. This outcome is consistent with 20 who attributed this improvement to the anti-inflammatory effect of the nanocurcumin and assumed that nanocurcumin can inhibit the neutrophil activation and aggregation.

Uses of nanocurcumin in group IV significantly lower the mean collagen fiber area percent when compared to that of CYP-treated group. These observations are in alignment with 24 who proved the ability of nanocurcumin to prevent the collagen deposition with subsequent fibrosis. The authors added that nanocurcumin can inhibit production of fibroblast and collagen formation.

The mean area percent of TNF-α in group IV was significantly lesser compared to that of CYP-treated group. These results agree with 25 & 20 who reported that the anti-inflammatory effect is facilitated by decreasing the production and releasing of factors of inflamation.

Additionally, using nanocurcumin in group IV significantly decrease the mean area percent of iNOS when compared to that of CYP-treated group. These findings agree with 22 who found that administration of curcumin nanoparticles could down-regulate expression levels of iNOS.

Biochemically, in the current research, it was observed that a significant reduction in the mean CK-MB in nanocurcumin group IV compared to that of CYP-treated group. These findings are in alignment with 26, 20 & 22 who attributed the decreased enzymatic level after nanocurcumin treatment to the cell membrane stabilizing and antioxidant potentials of nanocurcumin in addition to its ability to produce glutathione.

The mean GPx level in group IV statistically significant increased compared to CYP-treated group.That could explained by The ability of nanocurcumin to induce antioxidant capacity and antioxidant enzymes (CAT, GPx) besides the inhibition of oxidative stress 27.

According to 28, nanocurcumin is a natural antioxidant that can both enhance the activity of antioxidant enzymes like GPx and efficiently trap free radicals and endogenous oxidising active agents.

Also, there was statistically significant inhibition in the mean MDA results in group IV contrasted to CYP-treated group III. These results come in agreement with 20,27 & 29 who reported that the decrease in MDA level was due to the antioxidant effect and the anti-lipid peroxidation properties of nanocurcumin.

Conclusion

It could be concluded that cyclophosphamide (CYP) had negative consequences on the histological structure of the heart, cardiac enzymes, collagen fiber deposition and myofibroblast proliferation in

albino rats. Administration of nanocurcumin before or concomitantly with CYP injection could largely reduce these changes.

References:

1. Xiong, J., Ding, B., Zhu, W., Xu, L., & Yu, S. (2023): Exosomes from Adipose-Derived Mesenchymal Stem Cells Protect Against Cyclophosphamide-Induced Cardiotoxicity in Rats. International Heart Journal, 64(5), 935-944.
2. Alhowail, A. H., & Aldubayan, M. A. (2023): The Impact of Metformin on the Development of Hypothyroidism and Cardiotoxicity Induced by Cyclophosphamide, Methotrexate, and Fluorouracil in Rats. Pharmaceuticals, 16(9), 1312.
3. Gado, A. M., Adam, A. N. I., & Aldahmash, B. A. (2013): Cardiotoxicity induced by cyclophosphamide in rats: protective effect of curcumin. Journal of Research in Environmental Science and Toxicology, 2(4), 87-95.
4. Iqubal, A., Iqubal, M. K., Sharma, S., et al., (2019): Molecular mechanism involved in cyclophosphamide-induced cardiotoxicity: old drug with a new vision. Life sciences, 218, 112-131.
5. Flora, G., Gupta, D., & Tiwari, A. (2013): Nanocurcumin: a promising therapeutic advancement over native curcumin. Critical reviews™ in therapeutic drug carrier systems, 30.(4)
6. Karthikeyan, A., Senthil, N., & Min, T. (2020): Nanocurcumin: A Promising Candidate for Therapeutic Applications. Frontiers in pharmacology, 11, 487. https://doi.org/10.3389/fphar.2020.00487.
7. Madhana K., Mohan M., Meganathan P., et al., (2011): Effect of Dietary Fish Oil (Omega -3- Fatty Acid) Against Oxidative Stress in Isoproterenol Induced Myocardial Injury in Albino wistar Rats. Global Journal of Pharmacology. 5(1): 4-6.
8. Onaolapo, A.Y., Onaolapo, O.J., & Nwoha, P.U. (2017): methyl aspartylphenylalanine, the pons and cerebellum in mice: An evaluation of motor, morphological, biochemical, immunohistochemical and apoptotic. Journal of chemical neuroanatomy; 86:67-77.
9. Bashandy, M. A., & Zedan, O. I. (2019): Role of alpha lipoic acid on cyclophosphamide induced cardiotoxicity in adult male albino rat: histological study. Egyptian Journal of Histology, 42(4), 888-899.
10. Elrashidy, R. A., & Hasan, R. A. (2021): Cilostazol preconditioning alleviates cyclophosphamide-induced cardiotoxicity in male rats: Mechanistic insights into SIRT1 signaling pathway. Life sciences, 266, 118822. https://doi.org/10.1016/j.lfs.2020.118822.
11. Liu, Yunen., Tan, Dehong., Shi, Lin., et al., (2015): Blueberry Anthocyanins-Enriched Extracts Attenuate Cyclophosphamide-Induced Cardiac Injury. PLOS ONE. 10. e0127813. 10.1371/journal.pone.0127813.
12. Bhatt, L., Sebastian, B., & Joshi, V. (2017): Mangiferin protects rat myocardial tissue against cyclophosphamide induced cardiotoxicity. Journal of Ayurveda and integrative medicine, 8(2), 62–67. https://doi.org/10.1016/j.jaim.2017.04.006.
13. Cetik Yildiz., Songul., Ayhanci., et al., (2015): Protective Effect of Carvacrol Against Oxidative Stress and Heart Injury in Cyclophosphamide-Induced Cardiotoxicity in Rat. Brazilian Archives of Biology and Technology. 58. 569-576. 10.1590/S1516-8913201500022.
14. El-Agamy, D. S., Elkablawy, M. A., & Abo-Haded, H. M. (2017): Modulation of cyclophosphamide-induced cardiotoxicity by methyl palmitate. Cancer chemotherapy and pharmacology, 79(2), 399–409 .
15. Al-Hashmi, S., Boels, P. J., Zadjali, F., et al., (2012): Busulphan-cyclophosphamide cause endothelial injury, remodeling of resistance arteries and enhanced expression of endothelial nitric oxide synthase. PloS one, 7(1), e30897. https://doi.org/10.1371/journal.pone.0030897.
16. Song, Y., Zhang, C., Wang, C., et al., (2016): Ferulic Acid against Cyclophosphamide-Induced Heart Toxicity in Mice by Inhibiting NF-κB Pathway. Evidence-based complementary and alternative medicine: eCAM, 2016, 1261270. https://doi.org/10.1155/2016/1261270.
17. Nashwa, M. M. S., Abeer, R. H. M., Nagah, E. S. M. A., et al., (2019): The possible protective effect of Zingiber officinale extract on cyclophosphamide-induced cardiotoxicity in adult male albino rats. Journal of Toxicology and Environmental Health Sciences, 11(4), 38-49.
18. Omole, J. G., Ayoka, O. A., Alabi, Q. K., et al., (2018): Protective effect of kolaviron on cyclophosphamide-induced cardiac toxicity in rats. Journal of Evidence-Based Integrative Medicine, 23, 2156587218757649.
19. Potphode, N. D., Daunde, J. A., Desai, S. S., et al., (2018): Nano-curcumin: A potent enhancer of body antioxidant system in diabetic mice. Int. J. Phytomed, 10(3), 162-167.
20. Sarawi, W. S., Alhusaini, A. M., Fadda, L. M., et al., (2021): Nano-Curcumin Prevents Cardiac Injury, Oxidative Stress and Inflammation, and Modulates TLR4/NF-κB and MAPK Signaling in Copper Sulfate-Intoxicated Rats. Antioxidants (Basel, Switzerland), 10(9), 1414. https://doi.org/10.3390/antiox10091414.
21. Valizadeh, H., Abdolmohammadi-Vahid, S., Danshina, S., et al., (2020): Nano-curcumin therapy, a promising method in modulating inflammatory cytokines in COVID-19 patients. International immunopharmacology, 89, 107088.
22. Moutabian, H., Ghahramani-Asl, R., Mortezazadeh, T., et al., (2022): The cardioprotective effects of nano-curcumin against doxorubicin-induced cardiotoxicity: A systematic review. Biofactors.

23. Nahar, P. P., Slitt, A. L., & Seeram, N. P. (2015): Anti-Inflammatory Effects of Novel Standardized Solid Lipid Curcumin Formulations. Journal of medicinal food, 18(7), 786–792. https://doi.org/10.1089/jmf.2014.0053.
24. Kazemi-Darabadi, S., Nayebzadeh, R., Shahbazfar, A. A., et al., (2019): Curcumin and Nanocurcumin Oral Supplementation Improve Muscle Healing in a Rat Model of Surgical Muscle Laceration. Bulletin of emergency and trauma, 7(3), 292–299. https://doi.org/10.29252/beat-0703013.
25. Khadrawy, Y. A., Hosny, E. N., El-Gizawy, M. M., et al., (2021): The effect of curcumin nanoparticles on cisplatin-induced cardiotoxicity in male Wistar albino rats. Cardiovascular Toxicology, 21(6), 433-443.
26. Yadav, Y. C., Pattnaik, S., & Swain, K. (2019): Curcumin loaded mesoporous silica nanoparticles: assessment of bioavailability and cardioprotective effect. Drug Development and Industrial Pharmacy, 45(12), 1889-1895.
27. Mahlooji, M. A., Heshmati, A., Kheiripour, N., et al., (2022): Evaluation of Protective Effects of Curcumin and Nanocurcumin on Aluminium Phosphide Induced Subacute Lung Injury in Rats: Modulation of Oxidative Stress through SIRT1/FOXO3 Signalling Pathway. Drug Research, 72(02), 100-108.
28. Ibrahim, R. M., Elaal, F. E. Z. A. A., & Zaki, S. (2019): Effect of Curcumin and Nano-curcumin on Reduce Aluminum Toxicity in Rats. Int. J. Food Sci. Bioechnol, 4, 64.
29. Mohamed, M. A., El-Nahrawy, W. A., Zaher, A. M., et al., (2022): Therapeutic Role of Nanocurcumin Versus Monosodium Glutamate Toxicity. Egyptian Academic Journal of Biological Sciences, B. Zoology, 14(1), 55-65.